

## Supporting Information

### Mixed Solvent Exfoliated Transition Metal Oxides Nanosheets Based Flexible Solid State Supercapacitor Devices Endowed with High Energy Density

Shibsankar Dutta<sup>a</sup>, Shreyasi Pal<sup>b</sup> and Sukanta De<sup>a\*</sup>

<sup>a</sup>Department of Physics, Presidency University, 86/1 College Street, Kolkata-700073, India

<sup>b</sup>Department of Physics, Raidighi College, South 24 Parganas, Diamond Harbour Subdivision, Raidighi, West Bengal 743383, India

\*Corresponding Author

E-mail: [sukanta.physics@presiuniv.ac.in](mailto:sukanta.physics@presiuniv.ac.in)

#### Hansen solubility parameter (HSP) Study

The dissolution behavior can be explained by the Hansen solubility parameter (HSP) theory based on the three solubility parameters, these three dispersive ( $\delta_D$ ), polar ( $\delta_P$ ) and hydrogen bonding ( $\delta_H$ ) solubility parameters of solvent and solute are interrelated by the equation 1.

$$R_a = [4(\delta_{Dsolv} - \delta_{Dsolu})^2 + (\delta_{Psolv} - \delta_{Psolu})^2 + (\delta_{Hsolv} - \delta_{Hsolu})^2]^{\frac{1}{2}} \quad (1)$$

The solubility directly depends on the HSP distance ( $R_a$ ) value, smaller  $R_a$  value provides us higher solubility.

Mixed solvent exfoliation can also be explained by Hansen theory where each of three parameters is linear function of the volume fraction of the composition [equation 2].<sup>1</sup>

$$\delta_{blend} = \sum \phi_{n,comp} \delta_{n,comp} \quad (2)$$

Where  $\emptyset$  defines the volume fraction of each composition. Based on these two equations different solvent mixture can be predicted for the nano materials exfoliation.

### HSP value for solvent and TMOs:

Solvent	$\delta_D$ (MPa <sup>1/2</sup> )	$\delta_P$ (MPa <sup>1/2</sup> )	$\delta_H$ (MPa <sup>1/2</sup> )
Ethanol	15.8	8.8	19.4
Water	18.1	12.9	15.5
MoO <sub>3</sub>	16.6	18.04	10.23
MnO <sub>2</sub>	16.94	17.45	10.84
RuO <sub>2</sub>	16.94	17.45	10.84

### 1. Supporting Figures

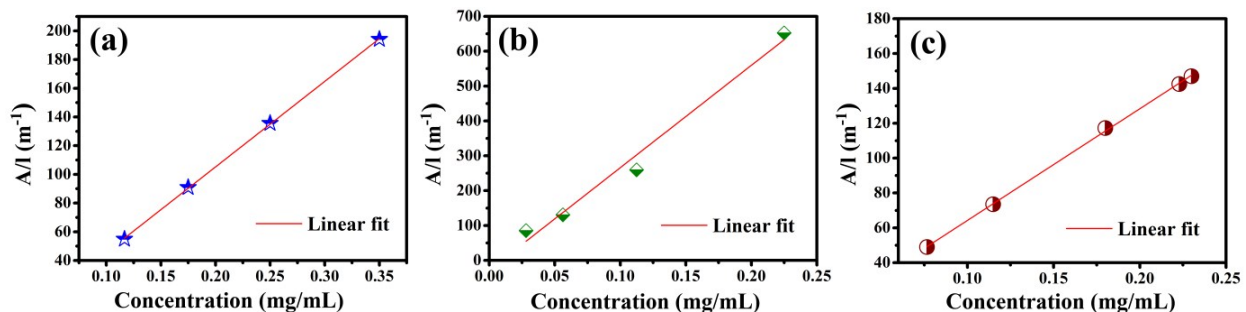


**Figure S1†** Absorbance per unit length ( $A/l$ ) vs concentration (a) MoO<sub>3</sub>, (b) MnO<sub>2</sub>, (c) RuO<sub>2</sub>.

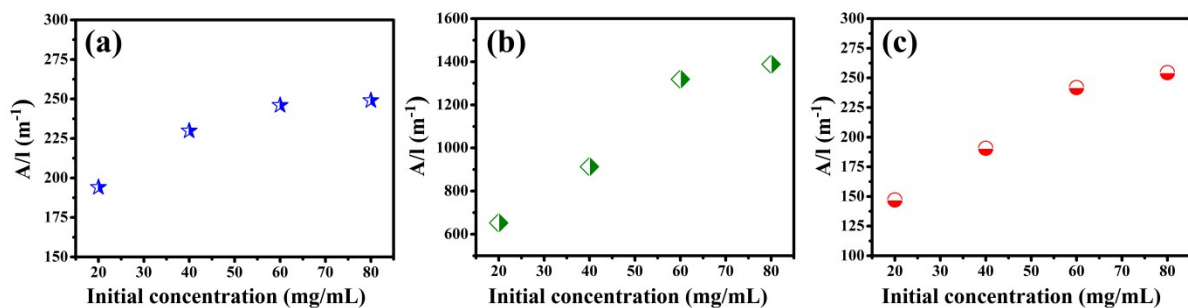


**Figure S2†** Absorbance per unit length ( $A/l$ ) vs initial concentration (a) MoO<sub>3</sub>, (b) MnO<sub>2</sub>, (c) RuO<sub>2</sub>.

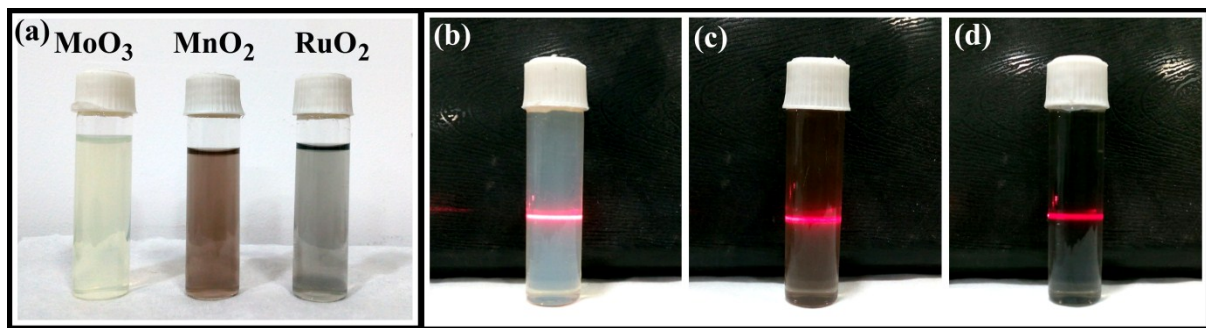


**Figure S3†** (a) Digital images of the MoO<sub>3</sub>, MnO<sub>2</sub> and RuO<sub>2</sub> nanosheets dispersion in Ethanol/ water, (b-d) Tyndall effect of the exfoliated MoO<sub>3</sub>, MnO<sub>2</sub> and RuO<sub>2</sub> nanosheets respectively.

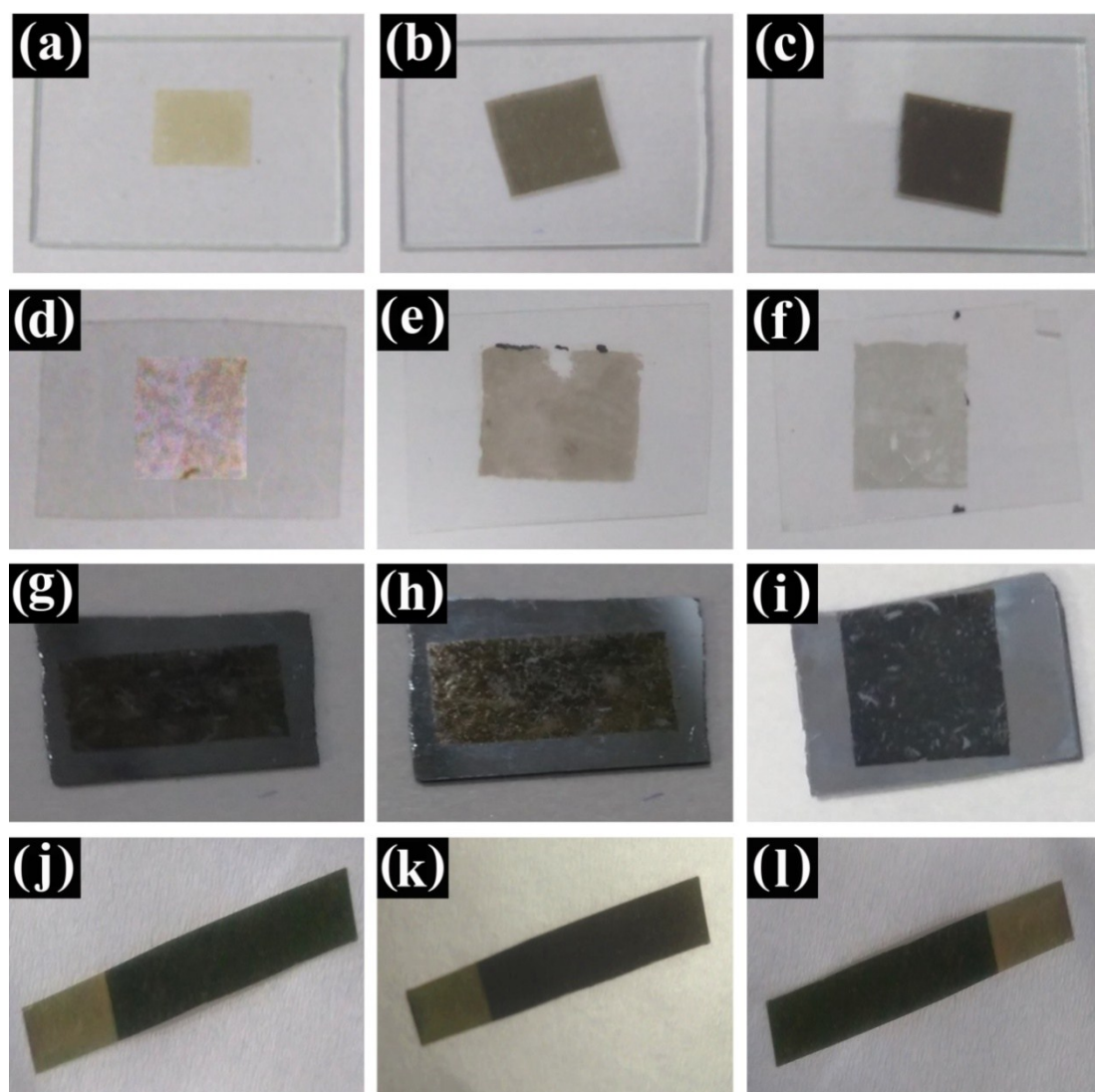


**Figure S4†** MoO<sub>3</sub>, MnO<sub>2</sub> and RuO<sub>2</sub> nanosheets thin films on (a-c) glass, (d-f) PET substrate respectively. MoO<sub>3</sub>/SWCNT, MnO<sub>2</sub>/SWCNT and RuO<sub>2</sub>/SWCNT nanocomposites thin films on (g-i) Si substrate and Au coated PET (j-l) substrate respectively.

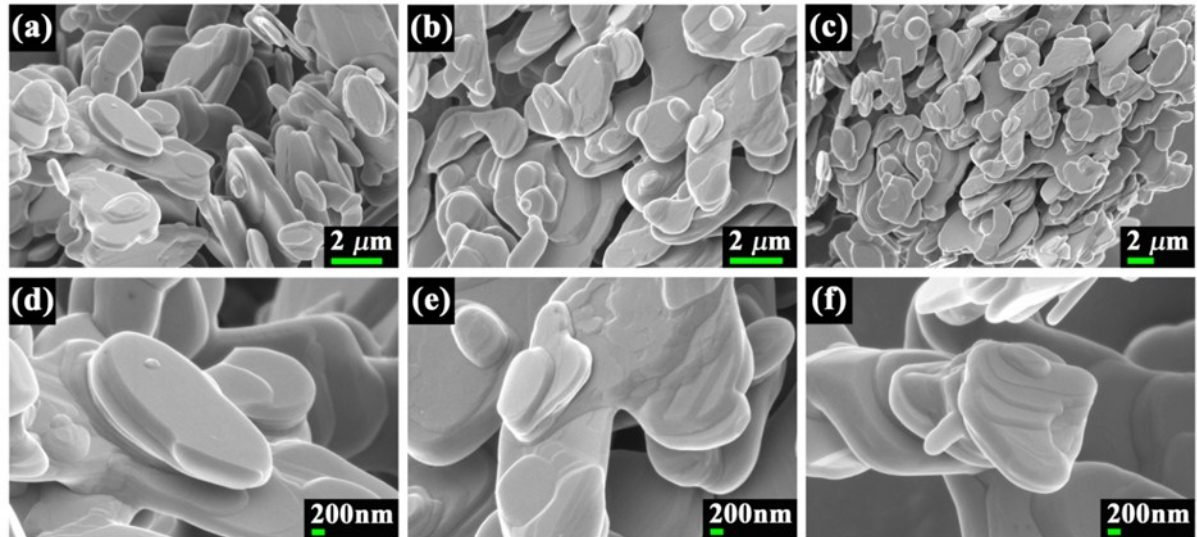


**Figure S5†** (a,b,c) FESEM images of the bulk MoO<sub>3</sub>, MnO<sub>2</sub>, RuO<sub>2</sub>; (d,e,f) showing their high magnification FESEM images respectively.

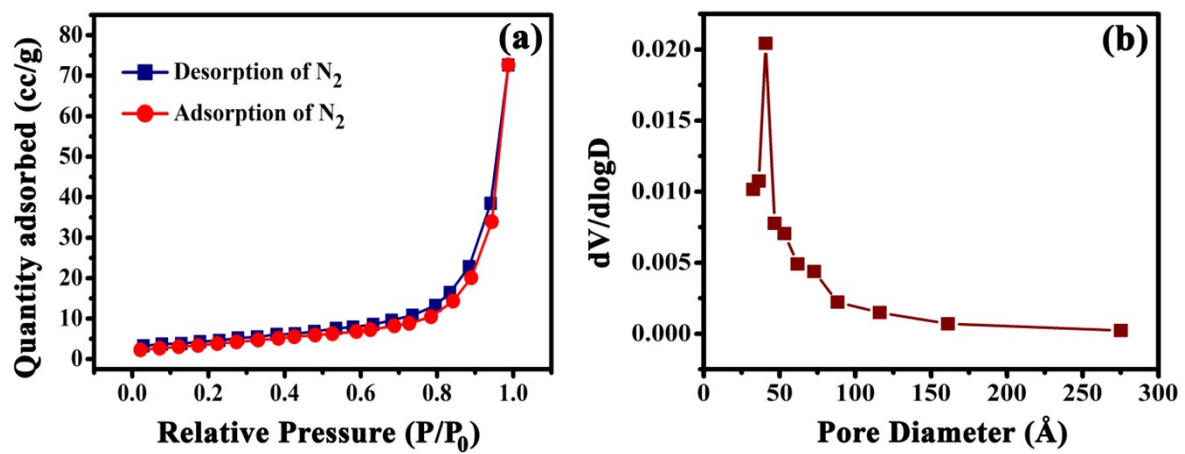


**Figure S6†** Nitrogen adsorption-desorption isotherm and corresponding pore size distribution curve of the pristine SWCNTs.

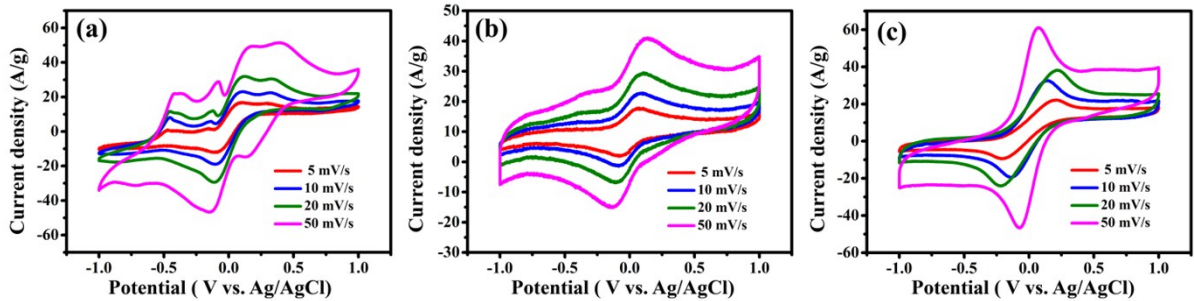


**Figure S7†** Cyclic voltammetry graph of (a) MoO<sub>3</sub>/SWCNT,(b) MnO<sub>2</sub>/SWCNT and (c) RuO<sub>2</sub>/SWCNT at different scan rates respectively using three electrode system.

## 2. Specific capacitance calculations:

In the case of two electrodes solid state supercapacitor the specific capacitance value was calculated using equation (3) and (4), where  $m_2$  was the total mass of the electrode materials,  $v$  (V/s) is the scan rate and  $\Delta t$  (sec) is the discharge time.<sup>2,3</sup> Energy density ( $E$ ) and power density ( $P$ ) can also be calculated from the equations (5) and (6).<sup>4</sup>

$$C = \frac{4 \int I_1 dV}{\nu m_2 \Delta V} \dots \dots \dots (3)$$

$$C = \frac{4I_2 \Delta t}{m_2 \Delta V} \dots \dots \dots (4)$$

$$E = \frac{1}{8} C(\Delta V)^2 \dots \quad (5)$$

$$P = \frac{1}{8} C \Delta V \nu \quad \dots \dots \dots \quad (6)$$

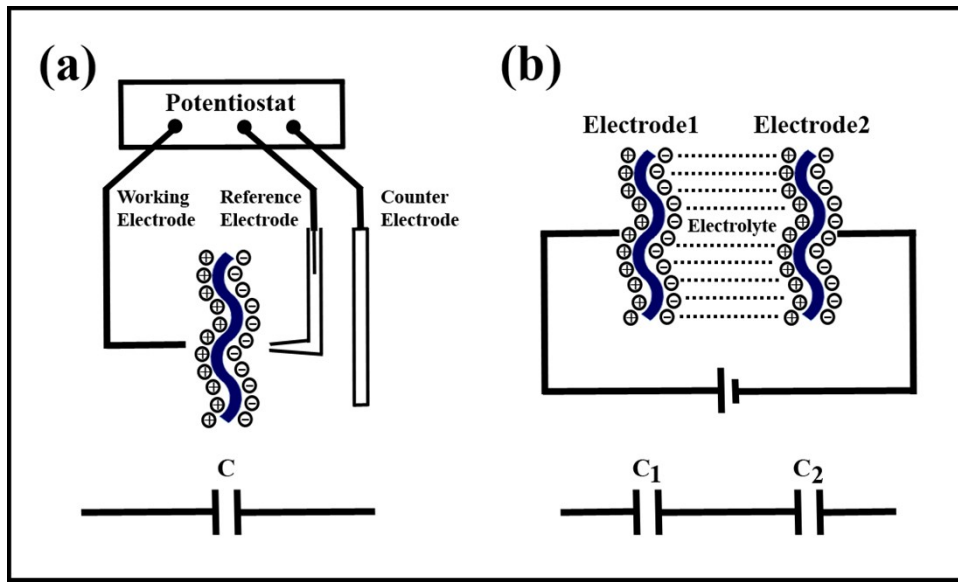


**Figure S8†** Schematic diagram and mechanism of the (a) three electrode and two electrode system.

Assuming the mass of the individual electrodes is  $m$ , the measured capacitance value for the two electrode system is:

$$c_{2E} = \frac{c}{2}$$

Where,  $c_1=c_2=c$

Therefore the specific capacitance value is:

$$c_{specific - 2E} = \frac{c_{2E}}{2m} = \frac{c}{4m}$$

In the case of three electrode system:

$$c_{3E} = c$$

Therefore the specific capacitance value is

$$c_{specific - 3E} = \frac{c_{3E}}{m} = \frac{c}{m}$$

The relation between the calculated specific capacitance value in the two and three electrode system is

$$c_{specific - 3E} = 4 \times c_{specific - 2E}$$

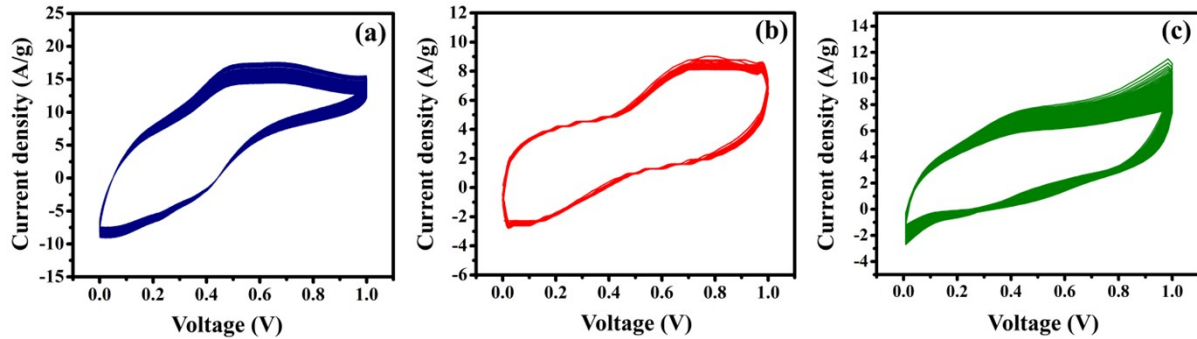


**Figure S9†** Cyclic voltammetry graph of (a) MoO<sub>3</sub>/SWCNT,(b) MnO<sub>2</sub>/SWCNT and (c) RuO<sub>2</sub>/SWCNT at 100 mV/s scan rates for 1000 cycles respectively using two electrode system.

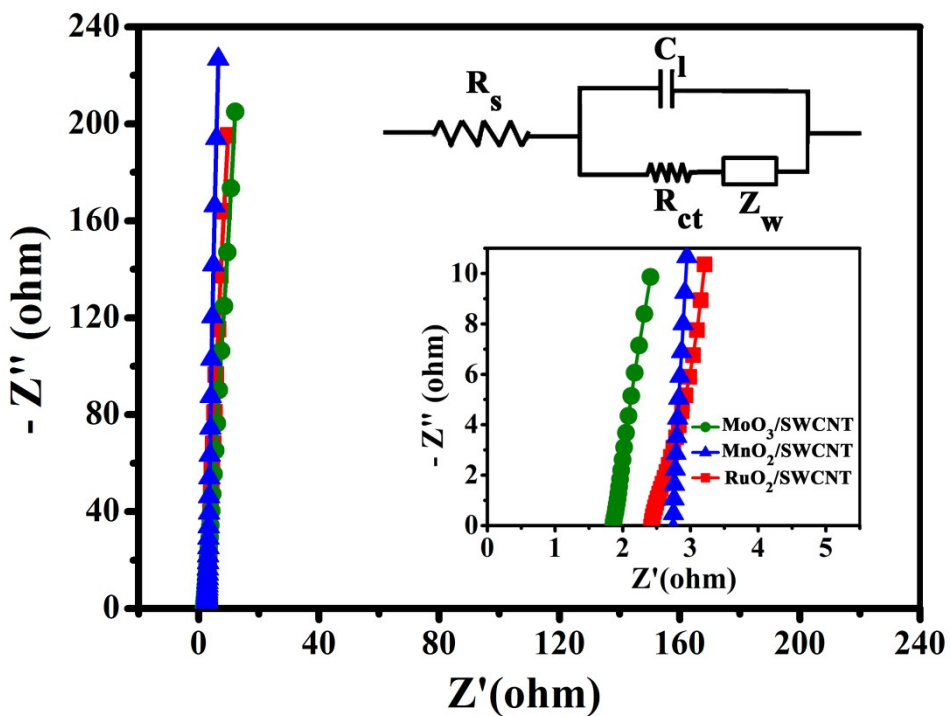
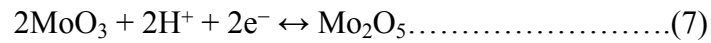


**Figure S10†** Nyquist plot of the all solid state supercapacitors; Inset showing the enlarge view of high frequency region and an equivalent circuit model.

### 3. The electrochemical behavior and charge discharge mechanism of the TMOs

According to the charge-storage mechanism the electrochemical reaction occurring at MoO<sub>3</sub>/SWCNT electrode is



The charge-storage mechanism of  $\text{MnO}_2/\text{SWCNT}$  electrode involves a reversible reduction/oxidation between  $\text{Mn}^{4+}$  and  $\text{Mn}^{3+}$ , which can be denoted as Eq. (8)



And the charge discharge mechanism of the RuO<sub>2</sub> can be explained by the reversible reactions given below

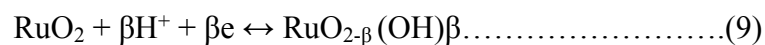


**Table S1. Comparison of the electrochemical performance of the TMOs/SWCNT supercapacitor with previously reported metal oxide supercapacitors.**

Electrode materials	Electrolyte	Specific capacitance (F/g)	Energy density (Wh kg <sup>-1</sup> )	Power density (kW kg <sup>-1</sup> )	Ref.
graphene/MnO <sub>2</sub> // graphene/Ag	-	-	7.53	90.3	5
3D Al@Ni@ MnOx nanospike// CCG	Na <sub>2</sub> SO <sub>4</sub> /PVA	-	23.02	0.947	6
MnO <sub>2</sub> @PANI// 3D graphene foam (GF)	KOH/PVA	95.3	37	0.386	7
Waste paper fibersRGO–MnO <sub>2</sub>	PVA/Na <sub>2</sub> SO <sub>4</sub>	220	19.6	2.4	8
MnO <sub>2</sub> nanoflakes	PVP/LiClO <sub>4</sub>	-	23	1.9	9
SWCNTs//RuO <sub>2</sub>	PVA/H <sub>3</sub> PO <sub>4</sub>	138	18.8	96	10
Graphene(IL-CMG)//RuO <sub>2</sub> -IL-CMG	PVA–H <sub>2</sub> SO <sub>4</sub>	175	19.7	6.8	11
MnO <sub>2</sub> //Mesoporous CNT	Na <sub>2</sub> SO <sub>4</sub>	85.8	47.4	0.200	12
Graphene/MnO <sub>2</sub> //Graphene	Na <sub>2</sub> SO <sub>4</sub>	31.0	30.4	0.100	13
Graphene/MnO <sub>2</sub> //ACF	Na <sub>2</sub> SO <sub>4</sub>	113.5	51.1	0.198	14
Activated graphene/MO <sub>2</sub> //Activated graphene	Na <sub>2</sub> SO <sub>4</sub>	175	32.3	21	15
Graphene/PANi//Graphene/RuO <sub>2</sub>	KOH	-	26.3	0.150	16
TiO <sub>2</sub> //CNT	LiPF <sub>6</sub>	-	12.5	0.300	17
Graphene/Ni(OH) <sub>2</sub> //Graphene/RuO <sub>2</sub>	KOH	-	48.0	0.230	18
Carbon spheres/MnO <sub>2</sub> //Carbon spheres	Na <sub>2</sub> SO <sub>4</sub>	-	22.1	0.100	19
CNT/MnO <sub>2</sub> //CNT/In <sub>2</sub> O <sub>3</sub>	Na <sub>2</sub> SO <sub>4</sub>	-	25.0	-	20
Graphene/MnO <sub>2</sub> //Graphene/MoO <sub>3</sub>	Na <sub>2</sub> SO <sub>4</sub>	307	42.6	0.276	21
MoO <sub>3</sub> /SWCNT// MoO <sub>3</sub> /SWCNT	PVA/H <sub>2</sub> SO <sub>4</sub>	717	24.89	1.61	Present Work
	1 M Na <sub>2</sub> SO <sub>4</sub> (Three electrode)	1205.08	669	21.69	
MnO <sub>2</sub> /SWCNT// MnO <sub>2</sub> /SWCNT	PVA/H <sub>2</sub> SO <sub>4</sub>	540	18.73	1.21	
	1 M Na <sub>2</sub> SO <sub>4</sub> (Three electrode)	1168.69	649.27	21.03	
RuO <sub>2</sub> /SWCNT// RuO <sub>2</sub> /SWCNT	PVA/H <sub>2</sub> SO <sub>4</sub>	676	23.48	1.52	
	1 M Na <sub>2</sub> SO <sub>4</sub> (Three electrode)	1308.45	726.91	23.55	

## Reference

1. K. G. Zhou, N. N. Mao, H. X Wang, Y. Peng and H. L. Zhang, *Angew. Chem. Int. Ed.*, 2011, **50**, 10839.
2. K. Zhou, W. Zhou, X. Liu, Y. Sang, S. Ji, W. Li, J. Lu, L. Li, W. Niu, H. Liu and S. Chen, *Nano Energy*, 2015, **12**, 510-520.
3. H. Wang, H. Yi, X. Chen and X. Wang, *J. Mater. Chem. A*, 2014, **2**, 3223-3230.
4. S.Ratha and C. S.Rout, *RSC Adv.*, 2015, **5**, 86551-86557.
5. Y. Shao, H. Wang, Q. Zhang and Y. Li, *J. Mater. Chem. C*, 2013, **1**, 1245-1251.
6. J. Yang, G. Li, Z. Pan, M. Liu, Y. Hou, Y. Xu, H. Deng, L. Sheng, X. Zhao, Y. Qiu and Y. Zhang, *ACS Appl. Mater. Interfaces*, 2015, **7**, 22172-22180.
7. K. Ghosh, C. Yue, M. Sk and R. Jena, *ACS Appl. Mater. Interfaces.*, 2017, **9**, 15350-15363.
8. H. Su, P. Zhu, L. Zhang, F. Zhou, G. Li, T. Li, Q. Wang, R. Sun and C. Wong, *J. Electroanal. Chem.*, 2017, **786**, 28-34.
9. P. Chen, H. Chen, J. Qiu and C. Zhou, *Nano Res.*, 2010, **3**, 594-603.
10. B. G. Choi, S. J. Chang, H. W. Kang, C. P. Park, H. J. Kim, W. H. Hong, S. Lee and Y. S. Huh, *Nanoscale*, 2012, **4**, 4983-4988.
11. J. Duay, E. Gillette, R. Liu and S. B. Lee, *Phys. Chem.*, 2012, **14**, 3329-3337.
12. H. Jiang, C. Li, T. Sun and J. Ma, *Nanoscale*, 2012, **4**, 807-812.
13. Z. S. Wu, W. D. Ren, W. Wang, F. Li, B. Liu and H. M. Cheng, *ACS Nano*, 2010, **4**, 5835-5842.
14. Z. Fan, J. Yan, T. Wei, L. Zhi, G. Ning, T. Li and F. Wei, *Adv. Funct. Mater.*, 2011, **21**, 2366-2375.

15. X. Zhao, L. Zhang, S. Murali, M. D. Stoller, Q. Zhang, Y. Zhu and R. S. Ruoff , *ACS Nano*, 2012, **6**, 5404-5412.
16. J. Zhang, J. Jiang, H. Li and X. S. Zhao, *Energy Environ. Sci.*, 2011, **4**, 4009-4015.
17. Q. Wang, Z. Wen and J. H. Li, *Adv. Funct. Mater.*, 2006, **16**, 2141-2146.
18. H. L. Wang, Y. Liang, T. Mirfakhrai, Z. Chen, H. S. Casalongue and H. J. Dai, *Nano Res.*, 2011, **4**, 729-736.
19. Z. Lei, J. Zhang and X. S. Zhao, *J. Mater. Chem.*, 2012, **22**, 153-160.
20. P. C. Chen, G. Shen, Y. Shi, H. Chen and X. Zhou, *ACS Nano*, 2010, **4**, 4403-4411.
21. J. Chang, M. Jin, F. Yao, T. H. Kim, V. T. Le, H. Yue, F. Gunes, B. Li, A. Ghosh, S. Xie, and Y. H. Lee, *Adv. Funct. Mater.*, 2013, **23**, 5074-5083.